Journal of the Taiwan Institute of Chemical Engineers 000 (2020) 1–7

Contents lists available at ScienceDirect

Journal of the Taiwan Institute of Chemical Engineers

journal homepage: www.elsevier.com/locate/jtice

Improved understanding of reaction kinetic identification problems using different nonlinear optimization algorithms

Zoltán Till*, Tibor Chován, Tamás Varga

Department of Process Engineering, University of Pannonia, 10, Egyetem Street, H-8200 Veszprém, Hungary

ARTICLE INFO

Article History:
Received 11 February 2020
Revised 22 April 2020
Accepted 24 May 2020
Available online xxx

Keywords:
Bias-variance tradeoff
Correlated kinetic parameters
Fixed-target optimization
Genetic algorithm
Kinetic model reduction
Metaheuristic search

ABSTRACT

The correct answer regarding which nonlinear optimization algorithm should we use for a given problem is that “it depends.” In this paper, we would like to add that “it depends, but use multiple programs whenever possible.” Here we consider 23 algorithms, implemented in MATLAB, evaluating their performance both on a lumped kinetic model for vacuum gas oil hydrocracking and a few-step kinetic model for ethane pyrolysis; the former particularly raised our interest as the kinetic parameters have no reference values in such models. We can use the results of such a study to estimate model variance; moreover, the statistical analysis of the identified minimum values can also quantify the parameter uncertainty. We can also identify key operating conditions where the applied kinetic model shows the highest sensitivity to the identified parameters, opening up the possibility to further reduce the uncertainty by targeting additional experimental work or by refining the identification problem.

1. Introduction

In the case of any engineering-related optimization problem, it is vital to select the best-suited algorithm in order to reach such a solution that can be reasonably applied during process design, debottlenecking, or scale-up. For example, Gomez-Gonzalez et al. modeled adsorption and used three different stochastic optimization routines to fit the adsorption isotherm parameters, here, a particle swarm algorithm stood out, because unlike the other methods, it gave a feasible solution every time [1]. However, the range of choice is quite extensive. Li et al. employed the Genetic Algorithm (GA) to identify the kinetics of the pyrolysis of fiberboards [2]. They suggested that the high computational demand of GA can be effectively countered by providing a good initial guess for the parameters using Kissinger’s method [3]; however, it is only applicable for thermogravimetric analysis. Ghahraloud and Farsi also used a genetic algorithm to optimize the heterocatalytic process of methanol oxidation [4]. Kumar and Balasubramanian utilized Particle Swarm Optimization, followed by a gradient-based step by the Levenberq-Marquardt algorithm for kinetic parameter estimation in case of hydrocracking of heavier petroleum feedstock [5]. Such combinations of heuristic and conventional search methods are promising to eliminate the randomness in the solution.

Therefore, the question arises from time to time on how to find the best-suited algorithm to solve a particular problem. Unfortunately, in most works dealing with algorithm comparison, only benchmark problems are used instead of the ones related to chemical engineering. Rios and Sahinidis provided an extensive comparison of more than 20 derivative-free solvers on convex and non-convex test problems, reaching a similar conclusion that there is no solver exist that dominates all the others [6]. Though overall they found the performance of some commercial solvers (that are not considered in this work) outstanding, there is a handful of solvers available on the public domain that performed well (e.g., PSwarm). There are other, less-extensive comparisons in the literature dealing with test problems available [7,8]. These also indicated that there is no single best choice.

In the case of kinetic identification problems (i.e., the particular scope of this work), it is much less common to use multiple algorithms on one problem and it is even rarer to compare them; usually, only the results of the leading algorithm are accepted, such as in the case of the VGO hydrocracking study of Zhang et al. [9]. Nevertheless, such works can be found, e.g., Baker et al. analyzed four popular global optimization methods in estimating the parameters of the upper part of glycolysis, emphasizing that balance has to be found between success and computational time [10]. Another good benchmark of optimization methods for kinetic parameter identification is the work of Villaverde et al. [11]. It only considers a limited number of methods but also deals with the scaling of the search variables, investigating the possible advantages of logarithmic scaling, showing that it has its advantages in the case of local and global optimization as well.

The solution of non-convex optimization problems (such as the kinetic identification problems considered in this paper) is likely to

* Corresponding author.
E-mail address: tillz@fmt.uni-pannon.hu (Z. Till).

https://doi.org/10.1016/j.jtice.2020.05.013

Abbreviations

c	concentration ([kmol m^{-3}] or [kg m^{-3}])
comp	component
E_a	activation energy [J mol^{-1}]
GHSV	gas hourly space velocity ([h^{-1}] or [s^{-1}])
k	reaction rate coefficient ([s^{-1}] or [m^3 mol^{-1} s^{-1}])
k_0	pre-exponential factor ([s^{-1}] or [m^3 mol^{-1} s^{-1}])
ℓ	dimensionless length [-]
LB	lower bound
LHSV	liquid hourly space velocity ([h^{-1}] or [s^{-1}])
N	number of observations
r	reaction rate [kmol m^{-3} s^{-1}]
$\underline{R_c}$	component source vector [kmol m^{-3} s^{-1}]
T	temperature ([°C] or [K])
υ	dimensionless linear flow velocity [s^{-1}]
UB	upper bound
$\underline{x}$	kinetic parameter vector
y	mass fraction [% (m/m)]

Greek letters

ε'	catalyst volume fraction [-]
η	catalyst efficiency factor [-]
μ	mean value
$\underline{\underline{\nu}}$	stoichiometric matrix
ρ	correlation coefficient
σ	standard deviation

Pseudocomponents

D	diesel
G	gaseous products
HN	heavy naphtha
K	kerosene
LN	light naphtha
VGO	vacuum gas oil

be non-unique. In other words, a finite set of experimental data can be fitted with multiple sets of adjustable parameter values [12]. It is possible to reformulate it to a convex optimization problem that in turn would have a unique global optimum [13,14]; nevertheless, such methods are less commonly used in the engineering practice due to their complexity. Alternatively, the application of statistical tools can be an effective way to compare the similar solutions [15].

The key idea of this paper is we can apply several different methods simultaneously to obtain valuable information regarding the nature of the solution of the kinetic parameter identification problems. Through two examples (a lumped kinetic model for vacuum gas oil hydrocracking and a few-step kinetic model for ethane pyrolysis), we highlight the several advantages of this approach. Firstly, model variance and total model error can be calculated. Secondly, the uncertainty of the model can be quantified. Thirdly, further experimental work can be targeted to reduce model uncertainty.

2. Investigated kinetic models

2.1. A lumped kinetic model for vacuum gas oil hydrocracking (VGO-15 and VGO-5)

The first kinetic model investigated in this paper is from the field of the so-called discrete lumping. The specific example is a lumped kinetic model for vacuum gas oil (VGO) hydrocracking, proposed by Sadighi and Reza Zahedi [16], consisting of 6 lumps (VGO, diesel (D), kerosene (K), heavy naphtha (HN), light naphtha (LN) and gaseous products (G)) and 15 (VGO-15) or 5 (VGO-5) reactions between them (Fig. 1). Reactions not present in the VGO-5 model are marked with dashed lines.

All details of the VGO hydrocracking model necessary for reproduction can be found in the Supplementary material. The reactor mass balance, given steady-state operation is:

$$\frac{d(\underline{c}\cdot\upsilon(\rho))}{d\ell} = \eta\cdot\varepsilon'\cdot\underline{R_c} \tag{1}$$

The component source vector, $\underline{R_c}$, can be calculated using the following equation:

$$\underline{R_c} = \underline{\underline{\nu}}\ \cdot\ \underline{r} \tag{2}$$

where $\underline{\underline{\nu}}$ is the stoichiometric matrix of the reaction network, and $\underline{r}$ is the reaction rate vector. Each reaction in $\underline{r}$ is modeled by a standard rate equation, where the reaction rate coefficient has an Arrhenius-type temperature dependency. Because of that, the reactor model becomes nonlinear. Component mass concentrations were available at four temperatures (380, 400, 410 and 420 °C) and four LHSV (0.5, 1, 1.5, 2 h^{-1}) levels.

Using a lumped kinetic model for benchmarking optimization algorithms is genuinely challenging because, unlike the standard problems, the location and value of the global minimum is unknown as the kinetic parameters have no reference values. Moreover, if we have two points whose difference in the objective function value is in the same range as the error of the measurement, it will become difficult to decide which one is correct. Here we would like to suggest that the solution with lower objective function value is not necessarily better, i.e., the problem has multiple global minima, even if the function values are not precisely the same.

2.2. A few-step kinetic model for ethane pyrolysis (ETP)

The second kinetic model considered here involves regular components. This model describes the gas-phase autocatalytic pyrolysis of ethane, studied extensively by Nurislamova et al. [17] and Snytnikov et al. [18]. The reaction network of the pyrolysis process is depicted in Table 1, with its size is comparable to the hydrocracking model with the 15 reactions. Furthermore, the reference values of the kinetic parameters are also available, making the performance evaluation of the optimization algorithms more straightforward.

The plug flow reactor model (similar to that in Eq. (1)), including all parameters necessary to reproduce the results, is included in the Supplementary material. Using the kinetic parameters from Table 1, data points were generated at eight temperature levels between 950

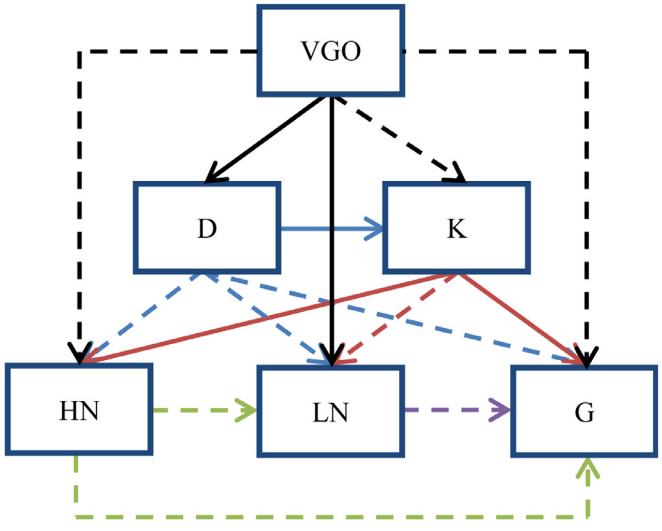

Fig. 1. Lumped kinetic network for VGO hydrocracking. Dashed lines indicate reactions only present in the VGO-15 model.

Please cite this article as: Z. Till et al., Improved understanding of reaction kinetic identification problems using different nonlinear optimization algorithms, Journal of the Taiwan Institute of Chemical Engineers (2020), https://doi.org/10.1016/j.jtice.2020.05.013

Table 1
List of reactions and kinetic parameters for the ethane pyrolysis model.

	Reaction	Pre-exponential factor [s^{-1} or $m^3\ mol^{-1}\ s^{-1}$]	Activation energy [$J\ mol^{-1}$]
1	$C_2H_6 \rightarrow CH_3\cdot + CH_3\cdot$	10^{16}	$3.6{\cdot}10^5$
2	$CH_3\cdot + C_2H_6 \rightarrow CH_4 + C_2H_5\cdot$	10^7	$5{\cdot}10^4$
3	$C_2H_5\cdot \rightarrow C_2H_4 + H\cdot$	$3.16{\cdot}10^{13}$	$1.7{\cdot}10^5$
4	$H\cdot + C_2H_6 \rightarrow H_2 + C_2H_5\cdot$	10^8	$4{\cdot}10^4$
5	$H\cdot + C_2H_4 \rightarrow C_2H_5\cdot$	$2.51{\cdot}10^7$	$8.4{\cdot}10^3$
6	$CH_3\cdot + C_2H_4 \rightarrow C_3H_7\cdot$	$7.94{\cdot}10^7$	$3.3{\cdot}10^4$
7	$C_3H_7\cdot \rightarrow CH_3\cdot + C_2H_4$	$7.94{\cdot}10^{13}$	$1.37{\cdot}10^5$
8	$C_2H_5\cdot + C_2H_5\cdot \rightarrow C_2H_4 + C_2H_6$	10^7	$8.4{\cdot}10^3$
9	$C_3H_7\cdot + C_2H_4 \rightarrow C_2H_5\cdot + C_3H_6$	$2.51{\cdot}10^4$	$2.76{\cdot}10^4$
10	$CH_3\cdot + C_2H_4 \rightarrow CH_4 + C_2H_3\cdot$	$3.98{\cdot}10^5$	$3.5{\cdot}10^4$
11	$CH_3\cdot + C_2H_3\cdot \rightarrow CH_4 + C_2H_2$	$8.91{\cdot}10^6$	$3.2{\cdot}10^3$
12	$C_2H_3\cdot + H\cdot \rightarrow C_2H_2 + H_2$	10^7	–
13	$C_2H_4 \rightarrow \cdot C_2H_4\cdot$	$6.31{\cdot}10^{15}$	$2.53{\cdot}10^5$
14	$\cdot C_2H_4\cdot + C_2H_6 \rightarrow CH_3\cdot + C_3H_7\cdot$	$5.01{\cdot}10^{11}$	$2.16{\cdot}10^5$
15	$\cdot C_2H_4\cdot \rightarrow C_2H_4$	$2.40{\cdot}10^5$	–

and 1020 K in 10 K increments and eight inflow velocity levels (corresponding to 0.05, 0.1, 0.2, 0.4, 0.7, 1, 1.6 and 2 s^{-1} GHSV values). The temperature and GHSV ranges were determined concerning the validation range of the kinetic model.

It is important to note that no noise was applied during data generation to keep the uncertainty of the ETP model as low as possible. This way, the global minimum of the identification problem (that measures the difference between the experimental and calculated data) will be zero because there is no residual error present.

3. The optimization target

The nonlinear optimization function to be minimized here describes the overall relative squared error between component yields from experiments and simulation as a function of the kinetic parameters of the reactions occurring between these components:

$$f(\underline{x}^n) = \sum_{T} \sum_{\substack{LHSV \\ GHSV}} \sum_{comp} \left(\frac{y_m - y_c}{y_m^{max}} \right)^2 \tag{3}$$

where the measured (m) and calculated (c) component mass fractions (y) are summarized over the different temperature levels (T), components (comp), and space velocities (LHSV or GHSV). y_m^{max} indicates the maximum measured concentration for a given component considering all temperature values and velocities. This type formulation of the identification problem performed well in the case of VGO hydrocracking in our previous work [19]; therefore, we have retained its use. We have also applied it in the case of the ETP model for the sake of simplicity and better comparison. Nevertheless, there are many options for an objective function to choose from and it certainly could affect the results. Siouris and Blakey compared nine different objective functions, evaluating their performance under a genetic algorithm in case of a kinetic identification problem and concluded that there are two main types of objective functions regarding whether we treat all component concentrations as equally important or not [20]. The case discussed here is the latter because we do not want the algorithm to "overlook" some species because of their low concentrations. Unfortunately, comparing 23 algorithms and multiple objective functions at the same time would be impracticable within a reasonable time.

For the formulation of the optimization problem, the lower and upper bounds of the kinetic parameters also to be defined as most algorithms deal with constrained problems. These are listed in the Supplementary material. In case of the ETP model, the constraints were defined following a preliminary sensitivity study starting from the reference values, whereas in case of the VGO hydrocracking models we mainly defined a wide radius based on the original values identified by Sadighi and Reza Zahedi [16], aiming to set the lower and upper bounds in a way that they will pose the smallest limitation as possible in practice.

It varies whether a specific algorithm can handle the different order of magnitude of the search variables. For the sake of simplicity, we used linearly normalized variables (x_n) between 0 and 1 (Eq (4)) to assure that this does not affect the convergence of the algorithms.

$$\underline{x}^{act} = \underline{x}^n \circ (\underline{UB} - \underline{LB}) + \underline{LB} \tag{4}$$

The kinetic identification problems discussed in this paper do not include more sophisticated linear and nonlinear constraints. Most of these algorithms cannot handle such problems; nevertheless, there would be some options available, even if not this many.

4. Identification methods

The algorithms discussed in this paper have been chosen based on the following aspects:

- It is considered as a global optimization method or a metaheuristic one. If not, it was already applied in solving kinetic parameter identification problems in the literature. For example, the Active-Set Optimization or Levenberg-Marquardt algorithm is widely used in such works [21].
- For the sake of simplicity, we have only considered such algorithms that have a compatible interface with the implemented kinetic models. In general, the aim is to draw attention to the fact that there are several programs which we can choose from to solve the optimization problem, and it is beneficial to apply more than one in parallel.

The final list of the algorithms is shown in Table 2. There are at least two things that were not essential in compiling this list. Firstly, although we intended to make a comprehensive overview and to take all major types of algorithms into consideration, Table 2 is not a review of all possible choices. Secondly, we did not deal with the novelty of these algorithms in terms of operations research. We are aware of the explosion in the field of "novel" metaheuristic algorithms, i.e., in some cases, only the nomenclature of the proposed algorithm shows some novelty, and any natural phenomenon could be an inspiration [22,23]. On the other hand, the main idea behind this paper is not to make a comparative study (mainly because the results would absolutely depend on the case studies), but to point out how the application of multiple algorithms gives a much better understanding of a given complex problem.

Please cite this article as: Z. Till et al., Improved understanding of reaction kinetic identification problems using different nonlinear optimization algorithms, Journal of the Taiwan Institute of Chemical Engineers (2020), https://doi.org/10.1016/j.jtice.2020.05.013

Table 2
List of nonlinear optimization algorithms considered for comparison.

Nr.	Name	Short name	Type
1	Active-Set Optimization [24]	active-set	derivative-based
2	Biogeography-Based Optimization [25]	BBO	evolutionary
3	Bees Algorithm [26]	BeA	swarm-based
4	Cultural Algorithm [27]	CA	evolutionary
5	Evolution Strategy with Covariance Matrix Adaptation [28]	CMA-ES	evolutionary
6	Controlled Random Search with local mutation [29]	CRS2	evolutionary
7	SCH Evolutionary Algorithm [30]	ESCH	evolutionary
8	Enhanced Scatter Search [31]	eSS	scatter search
9	Firefly Algorithm [32]	FA	swarm-based
10	Genetic Algorithm [33]	GA	evolutionary
11	Harmony Search [34]	HS	evolutionary
12	Interior Point Algorithm [35]	interior-point	derivative-based
13	Improved Stochastic Ranking Evolution Strategy [36]	ISRES	evolutionary
14	Levenberg-Marquardt [37]	LM	derivative-based
15	Nonlinear Optimization with Mesh Adaptive Direct Search [38]	NOMAD	direct search
16	MATLAB Particle Swarm Optimization [39]	particleswarm	swarm-based
17	Pattern Search [40]	patternsearch	direct search
18	Constrained Particle Swarm Optimization [41]	psopt	swarm-based
19	Particle Swarm Pattern Search [42]	PSwarm	swarm-based
20	Shuffled Complex Evolution [43]	SCE-UA	evolutionary
21	Constrained Simplex Method [44]	simplex	direct search
22	Simulated Annealing [45]	simulanneal	direct search
23	Sequential Quadratic Programming [46]	sqp	derivative-based

For the sake of keeping the size of the comparison study at bay, most options of these algorithms were left on their default values. This way, the "raw" efficiency of the algorithms can be compared. One exception is the sample size of the initial values that was standardized as 40 for the VGO-15 and VGO-5 models, and 100 for the ethane pyrolysis model. In the case of the algorithms that work with one initial value vector, that resulted in a multi-start approach using each initial value as a starting point. In the case of population-based algorithms, the sample size corresponds to the size of the initial population. Due to the stochastic nature of these algorithms, parallel runs were conducted starting from the same population. The number of parallel runs was chosen to be three and ten for the VGO and ETP models, respectively. In all cases, the result associated with the minimum objective function value was accepted.

5. Results and discussion

5.1. Reaching the optimization target

We compared the solutions of the applied optimization algorithms from a fixed-target viewpoint. A zero objective function value in Eq. (3) corresponds to a case where there is no residual error between the experimental and model results. It is not necessarily the goal to reach a zero value, especially if measurement noise is present, but this provides a joint reference, making the comparison of the results from different kinetic models possible. Fig. 2 shows the objective function values reached in the case of the VGO model as a function of the computational time, while Fig. 3 shows these values for the ETP model. For all kinetic models, there is a group of successful algorithms that can be separated from the others because they are

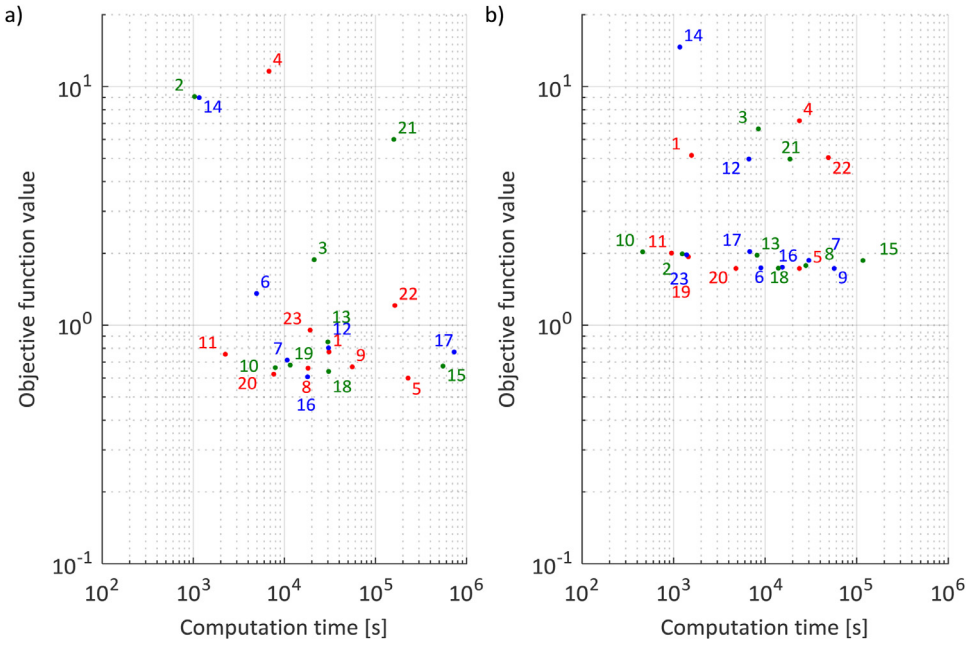

Fig. 2. Performance of different algorithms for VGO hydrocracking a) full reaction network b) reduced network.

Please cite this article as: Z. Till et al., Improved understanding of reaction kinetic identification problems using different nonlinear optimization algorithms, Journal of the Taiwan Institute of Chemical Engineers (2020), https://doi.org/10.1016/j.jtice.2020.05.013

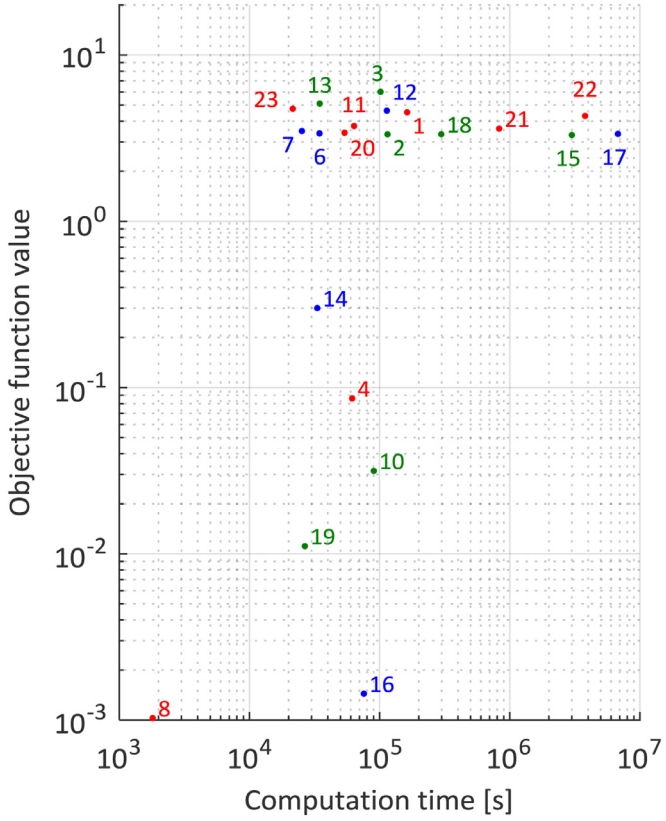

Fig. 3. Performance of different algorithms for ethane pyrolysis.

associated with significantly lower objective function values (an approximate value of 2 in the case of the VGO models, and below 1 in the case of the ETP model). Each successful solution of the optimization problem can be interpreted as a slightly different realization of the same kinetic model, but with different parameters.

It can be seen in Fig. 2 that noticeably more algorithms were successful in the case of the VGO-15 model and the associated objective function values are generally lower; on the other hand, the variance of the results is higher. This is a classic case of the bias-variance trade-off between the two models with different complexity. Hence, the total model error can be estimated. Assuming a normal distribution of the results from the successful runs, the errors are $f(\underline{x}^n) = 0.84 \pm 0.32$ and $f(\underline{x}^n) = 1.87 \pm 0.12$ for the full and the reduced reaction networks, respectively.

Fig. 3, which shows the performance of the algorithms in the case of the ETP model, is analogous to Fig. 2. Because here reaching $f(\underline{x}^n) = 0$ is a realistic target due to lack of measurement noise, the performance of the successful algorithms is associated with significantly lower objective function values. The number of successful algorithms (six), however, is significantly smaller than in the previous cases, mainly because second-order reactions are also present in the system, increasing its complexity. This is also the reason behind the higher computational time requirements, with the exception of the eSS (8) algorithm, indicating the advantages of combined global and local optimization approaches, as pointed out elsewhere [5]. The acceptable error level of the model is $f(\underline{x}^n) = 0.07 \pm 0.11$, in line with the expected target value.

As mentioned earlier, in the case of the VGO hydrocracking models, the location and the value of the global minimum are unknown. However, at this point, it can be suggested that the error level of the VGO-15 and VGO-5 models reported above quantifies the global minimum. Firstly, the size and nature of the optimization problems are very similar, i.e., they are kinetic identification problems with the same number of parameters to be identified for the ETP and VGO-15 model. Secondly, the complexity of the VGO-15 and VGO-5 models is lower. Given that the performance of the successful algorithms characterizes the global optimum in the case of the more complex ETP problem, it stands to reason to suggest that the estimated total error values of the VGO-15 and VGO-5 models also correspond to the global optimum. In conclusion, the application of different nonlinear optimization methods on the same kinetic identification problem provides a convenient way to estimate the location of the global minimum and the total model error with high certainty.

5.2. The importance of model reduction

As mentioned in Section 5.1, the VGO-15 model has a lower error but also higher variance. Fig. 2 only shows this in the case of the objective function values, but it is also worth examining how the identified kinetic parameter sets differ from each other. To that end, their correlation should be examined, because high correlation would indicate that the kinetic parameters obtained by the application of different GNLOPT algorithms are similar. The correlation coefficient of two kinetic parameters (denoted as A and B) can be calculated using the following equation:

$$\rho(A,B) = \frac{1}{N-1}\sum_{i=1}^{N}\left(\frac{A_i-\mu_A}{\sigma_A}\right)\left(\frac{B_i-\mu_B}{\sigma_B}\right) \tag{5}$$

where μ and σ are the mean and standard deviation of the parameters, and N is the number of observations (i.e., the number of kinetic parameter sets obtained in the successful runs). Graphical representations of the obtained correlation matrices in the case of the VGO-15 and VGO-5 models can be seen in Fig. 4. (Numerical values can be found in the Supplementary material.) Here, the tendency is the same as earlier, namely, the VGO-15 results show significantly higher variation; in fact, the correlation values are close to zero. This result is inconsistent with the very nature of the reaction network from Fig. 1 as the reactions should correlate through the concentrations of the component lumps. At the very least, the pre-exponential factors and activation energy values corresponding to the same reaction should be strongly correlated. The lack of this indicates high uncertainty in the identified kinetic parameters.

On the other hand, the correlation matrix of the kinetic parameters of the VGO-5 model in Fig. 4b has significantly higher values, in other words, the identified parameters have lesser uncertainty. This is an important result because lumped reaction networks are generally dense like the VGO-15 example. It is possible to identify the kinetic parameters of such networks so that the error of the model is reasonably low; nevertheless, the identified parameters would not be reliable, hindering the application of these models to solve reactor scale-up and design problems. Instead, it is important to reduce the reaction network to keep the uncertainties in the model as low as possible.

5.3. Differences between the identified kinetic parameters

So far only the overall performance of the identified kinetic parameters has been evaluated based on Eq. (3). For example, there were 16 successful optimization methods in the case of the VGO-5 model in Fig. 2b, associated with approximately the same objective function values. In addition, it is worth to investigate the possible difference between the results more in-depth. An effective way to do that is to compute the difference between the concentration profiles obtained using the identified kinetic parameters. The standard deviation of the simulated pseudocomponent mass concentrations was calculated in case of the VGO-5 model (using the ESCH, eSS, GA, HS, NOMAD, and PSwarm algorithms) by the following equation:

Please cite this article as: Z. Till et al., Improved understanding of reaction kinetic identification problems using different nonlinear optimization algorithms, Journal of the Taiwan Institute of Chemical Engineers (2020), https://doi.org/10.1016/j.jtice.2020.05.013

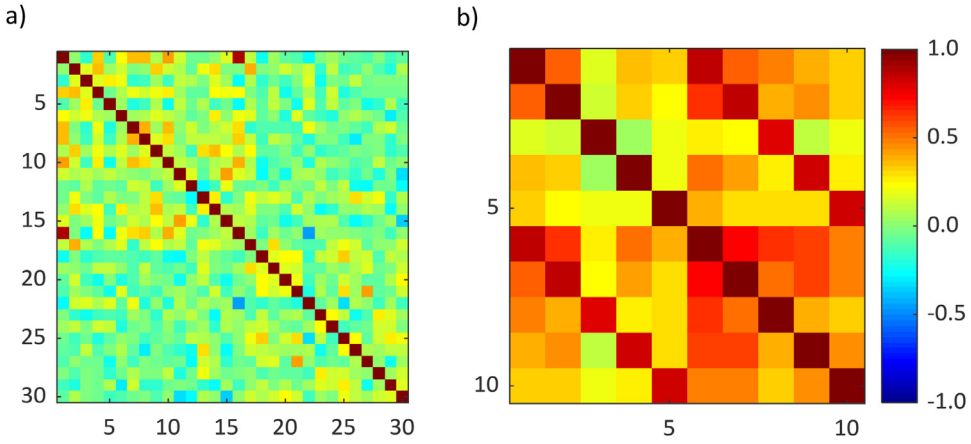

Fig. 4. Correlation between the identified parameters in the case of the a) VGO-15 and b) VGO-5 model.

$$\sigma = \sqrt{\frac{1}{N-1}\sum_{i=1}^{N}\left(y_i^c - \frac{1}{N}\sum_{j=1}^{N} y_j^c\right)^2} \quad (6)$$

where N is the number of observations, i.e., the number of calculated mass concentrations from each global minimum at a given temperature and LHSV value. The resulting standard deviations are shown in Fig. 5a in the case of VGO, where the highest values were obtained. It can be seen that even though the value of the objective function is nearly the same, the calculated mass concentrations can differ considerably under certain operating conditions. Fig. 5b shows this difference at LHSV = 0.5 h^{-1}. Apparently, that even low standard deviation can represent a high bias from the measured value, as is the case at 400 °C.

This type of investigation also highlights the possible experimental conditions where further measurements would be advantageous [47]. For example, the measured value at 400 °C (or alternatively, at 380 °C) seems to be not in line with the other data points, therefore, carrying out the hydrocracking experiment at these temperature levels anew, and subsequently identifying of the kinetic parameters would enhance the performance of the kinetic model. This is a further advantage of the application of multiple algorithms during the kinetic parameter identification.

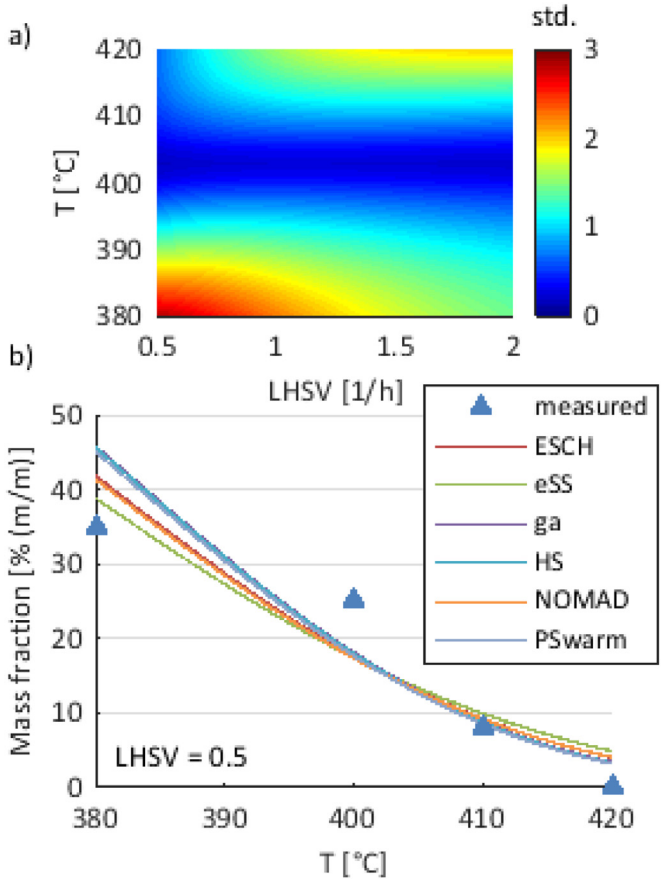

Fig. 5. VGO concentration obtained using different kinetic parameters a) Standard deviation b) Measured and calculated values.

6. Conclusions and next steps

Studies assessing the performance of nonlinear optimization algorithms in kinetic model identification are scarce in the literature, and the reason behind this is simple: there is no one "best" algorithm for all cases. Even in the case of the three identification problems discussed here, some algorithms performed well in one case and not so well in the other. On the other hand, we think imperative to provide some guidelines for non-mathematicians dealing with similar problems which algorithms to choose from. The answer is simple but peculiar on second thought: never choose only one. Applying completely different NLP solvers to the same problems might as well provide valuable insight into the problem regarding the uncertainty of the solution or even of the whole model. In the next step, we would like to quantify the latter further, especially how the relations between similar minima describes the variance of the given model. It appears to be equally interesting to find out how the characteristic of the objective function contributes to the uncertainty of the solution of the identification problem. Still, the most important thing is to keep the practical approach in mind.

Declaration of Competing Interest

None.

Acknowledgment

We acknowledge the financial support of Széchenyi 2020 under the GINOP-2.3.2–15–2016–00053. Tamás Varga's contribution to this paper was supported by the Janos Bolyai Research Scholarship of the Hungarian Academy of Sciences.

Please cite this article as: Z. Till et al., Improved understanding of reaction kinetic identification problems using different nonlinear optimization algorithms, Journal of the Taiwan Institute of Chemical Engineers (2020), https://doi.org/10.1016/j.jtice.2020.05.013

Supplementary materials

Supplementary material associated with this article can be found in the online version at doi:10.1016/j.jtice.2020.05.013.

References

[1] Gomez-Gonzalez R, Cerino-Córdova FJ, Garcia-León AM, Soto-Regalado E, Davila-Guzman NE, Salazar-Rabago JJ. Lead biosorption onto coffee grounds: comparative analysis of several optimization techniques using equilibrium adsorption models and ANN. J Taiwan Inst Chem Eng 2016;68:201–10. doi: 10.1016/j.jtice.2016.08.038.
[2] Li K-Y, Huang X, Fleischmann C, Rein G, Ji J. Pyrolysis of medium-density fiberboard: optimized search for kinetics scheme and parameters via a genetic algorithm driven by Kissinger's method. Energy Fuels 2014;28:6130–9. doi: 10.1021/ef501380c.
[3] Kissinger HE. Reaction Kinetics in Differential Thermal Analysis. Anal Chem 1957;29:1702–6. doi: 10.1021/ac60131a045.
[4] Ghahraloud H, Farsi M. Modeling and optimization of methanol oxidation over metal oxide catalyst in an industrial fixed bed reactor. J Taiwan Inst Chem Eng 2017;81:95–103. doi: 10.1016/j.jtice.2017.10.003.
[5] Kumar V, Balasubramanian P. Kinetic parameter estimation in hydrocracking using hybrid particle swarm optimization. Fuel 2009;88:2171–80. doi: 10.1016/j.fuel.2009.05.004.
[6] Rios LM, Sahinidis NV. Derivative-free optimization: a review of algorithms and comparison of software implementations. J Glob Optim 2013;56:1247–93. doi: 10.1007/s10898-012-9951-y.
[7] Civicioglu P, Besdok E. A conceptual comparison of the Cuckoo-search, particle swarm optimization, differential evolution and artificial bee colony algorithms. Artif Intell Rev 2013;39:315–46. doi: 10.1007/s10462-011-9276-0.
[8] Hansen N, Auger A, Ros R, Finck S, Pošík P. Comparing results of 31 algorithms from the black-box optimization benchmarking BBOB-2009. In: Proceedings of the 12th Annual Conference on Genetic and Evolutionary Computation GECCO 10. Portland, Oregon, USA. ACM Press; 2010. p. 1689. doi: 10.1145/1830761.1830790.
[9] Zhang T, Leyva C, Froment GF, Martinis J. Vacuum gas oil hydrocracking on NiMo/USY zeolite catalysts. Experimental study and kinetic modeling. Ind Eng Chem Res 2015;54:858–68. doi: 10.1021/ie503567b.
[10] Baker SM, Schallau K, Junker BH. Comparison of different algorithms for simultaneous estimation of multiple parameters in kinetic metabolic models. J Integr Bioinform 2010. doi: 10.2390/biecoll-jib-2010-133.
[11] Villaverde AF, Froehlich F, Weindl D, Hasenauer J, Banga JR. Benchmarking optimization methods for parameter estimation in large kinetic models. BioRxiv 2018. doi: 10.1101/295006.
[12] Stitt H, Marigo M, Wilkinson S, Dixon T. How Good is Your Model? Johns Matthey Technol Rev 2015;59:74–89. doi: 10.1595/205651315X686804.
[13] Al-Matouq A, Vincent T. A convex optimization framework for the identification of homogeneous reaction systems. Automatica 2020;114:108823. doi: 10.1016/j.automatica.2020.108823.
[14] Rodrigues D, Billeter J, Bonvin D. Global identification of kinetic parameters via the extent-based incremental approach. Comput Aided Chem Eng 2017;40:2119–24. doi: 10.1016/B978-0-444-63965-3.50355-X.
[15] Ayyıldız M, Çetinkaya K. Comparison of four different heuristic optimization algorithms for the inverse kinematics solution of a real 4-DOF serial robot manipulator. Neural Comput Appl 2016;27:825–36. doi: 10.1007/s00521-015-1898-8.
[16] Sadighi S, Reza Zahedi G. Comparison of kinetic-based and artificial neural network modeling methods for a pilot scale vacuum gas oil hydrocracking reactor. Bull Chem React Eng Catal 2013;8. doi: 10.9767/bcrec.8.2.4722.125-136.
[17] Nurislamova LF, Stoyanovskaya OP, Stadnichenko OA, Gubaidullin IM, Snytnikov VN, Novichkova AV. Few-step kinetic model of gaseous autocatalytic ethane pyrolysis and its evaluation by means of uncertainty and sensitivity analysis. Chem Prod Process Model 2014;9. doi: 10.1515/cppm-2014-0008.
[18] Snytnikov VN, Mischenko TI, VlN S, Chernykh IG. A reactor for the study of homogeneous processes using laser radiation energy. Chem Eng J 2009;150:231–6. doi: 10.1016/j.cej.2009.02.028.
[19] Till Z, Varga T, Szabó L, Chován T. Identification and observability of lumped kinetic models for vacuum gas oil hydrocracking. Energy Fuels 2017;31:12654–64. doi: 10.1021/acs.energyfuels.7b02040.
[20] Siouris S, Blakey S. Fitness functions for evolutionary optimization of rate parameters in chemically reacting systems. Chem Eng Sci 2019;196:354–65. doi: 10.1016/j.ces.2018.11.009.
[21] Rani KNP, Neeharika TSVR, Kumar TP, Satyavathi B, Ch Sailu, Prasad RBN. Kinetics of enzymatic esterification of oleic acid and decanol for wax ester and evaluation of its physico-chemical properties. J Taiwan Inst Chem Eng 2015;55:12–6. doi: 10.1016/j.jtice.2015.04.011.
[22] Sörensen K. Metaheuristics-the metaphor exposed. Int Trans Oper Res 2015;22:3–18. doi: 10.1111/itor.12001.
[23] Weyland D. A critical analysis of the harmony search algorithm—How not to solve Sudoku. Oper Res Perspect 2015;2:97–105. doi: 10.1016/j.orp.2015.04.001.
[24] Powell MJD. Variable metric methods for constrained optimization. In: Bachem A, Korte B, Grötschel M, editors. Mathematical Programming the State of the Art. Berlin, HeidelbergBerlin Heidelberg: Springer; 1983. p. 288–311. doi: 10.1007/978-3-642-68874-4_12.
[25] Simon D. Biogeography-based optimization. IEEE Trans Evol Comput 2008;12:702–13. doi: 10.1109/TEVC.2008.919004.
[26] Pham DT, Ghanbarzadeh A, Koc E, Otri S, Rahim S, Zaidi M. The Bees algorithm. United Kingdom: manufacturing engineering centre. Cardiff University; 2005.
[27] Reynolds RG. An introduction to cultural algorithms. In: Proceedings of the Third Annual Conference on Evolutionary Programming. River Edge. NJ: World Scientific Publishing Co. Pte. Ltd.; 1994. p. 131–9.
[28] Hansen N, Ostermeier A. Completely derandomized self-adaptation in evolution strategies. Evol Comput 2001;9:159–95. doi: 10.1162/106365601750190398.
[29] Price WL. Global optimization by controlled random search. J Optim Theory Appl 1983;40:333–48. doi: 10.1007/BF00933504.
[30] da Silva Santos CH, Goncalves MS, Hernandez-Figueroa HE. Designing novel photonic devices by bio-inspired computing. IEEE Photonics Technol Lett 2010;22:1177–9. doi: 10.1109/LPT.2010.2051222.
[31] Egea JA, Martí R, Banga JR. An evolutionary method for complex-process optimization. Comput Oper Res 2010;37:315–24. doi: 10.1016/j.cor.2009.05.003.
[32] Yang X-S. Nature-inspired metaheuristic algorithms. 2. ed Frome: Luniver Press; 2010.
[33] The Mathworks, Inc. How the Genetic Algorithm Works. MATLAB Doc2019. https://www.mathworks.com/help/gads/how-the-genetic-algorithm-works.html (accessed January 29, 2020).
[34] Geem ZW, Kim JH, Loganathan GV. A new heuristic optimization algorithm: Harmony search. SIMULATION 2001;76:60–8. doi: 10.1177/003754970107600201.
[35] Byrd RH, Hribar ME, Nocedal J. An interior point algorithm for large-scale nonlinear programming. SIAM J Optim 1999;9:877–900. doi: 10.1137/S1052623497325107.
[36] Runarsson TP, Yao X. Search biases in constrained evolutionary optimization. IEEE Trans Syst Man Cybern Part C Appl Rev 2005;35:233–43. doi: 10.1109/TSMCC.2004.841906.
[37] Moré JJ. The Levenberg-Marquardt algorithm: implementation and theory editor. In: Watson GA, editor. Numerical Analysis, 630. Berlin, Heidelberg: Springer Berlin Heidelberg; 1978. p. 105–16. doi: 10.1007/BFb0067700.
[38] Le Digabel S. Algorithm 909: NOMAD: nonlinear optimization with the MADS algorithm. ACM Trans Math Softw TOMS 2011;37:44.
[39] Kennedy J, Eberhart R. Particle swarm optimization. In: Proceedings of the ICNN95 International Joint Conference on Neural Networks. Perth, WA, Australia. IEEE; 1995. p. 1942–8. doi: 10.1109/ICNN.1995.488968.
[40] Audet C, Dennis JE. Analysis of generalized pattern searches. SIAM J Optim 2002;13:889–903. doi: 10.1137/S1052623400378742.
[41] Birge B. PSOt - a particle swarm optimization toolbox for use with Matlab. In: Proceedings of the 2003 IEEE Swarm Intelligence Symposium SIS03 Cat No03EX706. Indianapolis, Indiana, USA: IEEE; 2003. p. 182–6. doi: 10.1109/SIS.2003.1202265.
[42] Vaz AIF, PSwarm VLN. a hybrid solver for linearly constrained global derivative-free optimization. Optim Methods Softw 2009;24:669–85. doi: 10.1080/10556780902909948.
[43] Duan Q, Sorooshian S, Gupta V. Effective and efficient global optimization for conceptual rainfall-runoff models. Water Resour Res 1992;28:1015–31. doi: 10.1029/91WR02985.
[44] D'Errico J. fminsearchbnd, fminsearchcon. MathWorks File Exch2012. https://www.mathworks.com/matlabcentral/fileexchange/8277-fminsearchbnd-fminsearchcon (accessed January 29, 2019).
[45] Černý V. Thermodynamical approach to the traveling salesman problem: an efficient simulation algorithm. J Optim Theory Appl 1985;45:41–51. doi: 10.1007/BF00940812.
[46] Nocedal J, Wright S. Numerical optimization. New York: Springer; 2006. doi: 10.1007/978-0-387-40065-5.
[47] Banga JR, Balsa-Canto E. Parameter estimation and optimal experimental design. Essays Biochem 2008;45:195–210. doi: 10.1042/bse0450195.

Please cite this article as: Z. Till et al., Improved understanding of reaction kinetic identification problems using different nonlinear optimization algorithms, Journal of the Taiwan Institute of Chemical Engineers (2020), https://doi.org/10.1016/j.jtice.2020.05.013